RESEARCH

17(48), 2020

ISSN 2319–7757 EISSN 2319–7765

Indian Journal of Engineering

Specific characteristics and microstructure of Portland cement pastes containing wheat straw ash (WSA)

H.H.M. Darweesh

Refractories, Ceramics and Building Materials Department, National Research Centre, Cairo, Egypt
Email: hassandarweesh2000@yahoo.com

Article History
Received: 29 September 2020
Accepted: 14 November 2020
Published: November 2020

Citation
Darweesh HHM. Specific characteristics and microstructure of Portland cement pastes containing wheat straw ash (WSA). *Indian Journal of Engineering*, 2020, 17(48), 569-583

General Note
Article is recommended to print as color digital version in recycled paper.

ABSTRACT

Utilization of wheat straw ash (WSA), which is one of the most abundant, renewable and green supplementary cementitious materials to minimize the environmental pollution and also the CO_2 emission. In the current research work, the influence of WSA on the physical, chemical and mechanical properties of hydrated cement pastes incorporated different ratios of WSA up to 90 days was investigated. Results showed that the fineness of the different cement composites increased with the incorporation of WSA. The water of consistency as well as setting times (Initial and final) decreased with WSA content. The bound water content, bulk density and compressive strength were improved and enhanced with the increase of WSA content only up to 16 wt. % WSA, and then decreased, but the $Ca(OH)_2$ content and bulk density were reduced. The obtained results of the newly formed hydration products were confirmed by measuring the heat of hydration and DTA curves. The heat f hydration increased with WSA content indicating the increase of hydration rate. It is concluded that the cement could be partially replaced by WSA without any adverse response on the properties of cement pastes. The free lime content was gradually reduced with the increase of WSA ratio as shown by the Diffrential Thermal Analysis (DTA). So, the WSA acts as a pozzolanic and also a filling material. The SEM images showed that the existence of WSA with the cement phases reflected positively on the microstructure of the cement phases.

Keywords: Cement, wheat straw ash, heat of hydration, setting, free lime, density, porosity, strength, DTA.

1. INTRODUCTION

1.1. Scope of the problem

Nanotechnology is to make materials less than 100 nm, i.e. nanomaterials to convert it into nanoparticles with essentially new and very fine features and functions [1-4]. The very important request and need of nanotechnology is one of the most interesting processes because it could be used in all applied science branches as: physics, chemistry, materials sciences, biology, agriculture, medicine, tissue engineering, bones scaffolds, dentistery, cement technology, ceramics, nanoceramics, bioceramics and in a general biomaterials because the nanoparticles are highly effective additives for the modification of cement products, even at small ratios. The author interests with using nanomaterials or accurately nanoparticles to prepare cement batches containing ultra fine and nano raw materials as nano-SiO_2 and nano-Al_2O_3 to indicate the importance of nano particles, to improve the physical, chemical and mechanical properties, and also the durability of the resulting hydrating products against aggressive environments. Recently, nanomaterials are the basis and backbone of nanotechnology [3,4].

In many agricultural countries like Egypt, Sudan, Tunisia, China and India, emissions of gaseous and particulate pollutants from open burning of agricultural residues are one of the most important sources of air pollution [5]. The biomass power plant, among other alternatives, is widely used for the disposal of biomass wastes, in order to solve the environmental problems [6]. Accordingly, the wheat straw (WS) is often containing much more active silica and alumina which helps and possesses a good pozzolanic activity with the evolved Ca $(OH)_2$ that produced from the hydration of calcium silicate phases of the cement (C_3S and β-C_2S), and so it can be potentially reused as a supplementary cementitious material to partially replace cement, gradually [7-11]. Previous works [12-17] had reported that the addition of traditional supplementary cementitious materials could improve the physical, chemical and mechanical properties, and also durability.

1.2. Objectives of the work

The main objectives of this work are the evaluation and following the characteristics of Ordinary Portland cement incorporating wheat straw ash hydrated up to 90 days. The heat of hydration, setting, free lime, density, porosity and strength were studied at all hydration times. The obtained results were confirmed with Differential thermal analysis (DTA) and scanning electron microscopy (SEM).

2. EXPERIMENTAL

2.1. Materials

The used materials in this investigation are Ordinary Portland cement (OPC) with fineness 3400 cm^2/g, and waste of wheat straw (WS) as a source of nanosilica with fineness 6010 cm^2/g. The fineness was carried out using "Air Permeability Apparatus". The OPC sample was taken from Sakkara cement factory, Giza, Egypt. The commercial name of used OPC cement is known as "Asmant El-Momtaz", while WS sample was provided from a local plant, Giza, Egypt. The WS sample was first processed and washed with running water, and also with distilled water, and then let to dry under sun and open air for few days. The dried SFS was subjected for firing at 700 ºC inside a suitable muffle furnace for two hours soaking time to produce what is known as wheat stalk ash (WSA). Then, the resulting WSA was screened to pass through 300 µm standard sieve. The chemical composition of the OPC and WSA measured by X-ray florescence technique (XRF) is shown in Table 1. The mineralogical phase composition of the used OPC as calculated from Bogue equations [16,17] is given in Table 2, while the mix composition is illustrated in Table 3. The WSA particles are amorphous and crystalline and it is mainly composed of a large percentage of nano-SiO_2 and a lower percentage of nano-Al_2O_3.

Table 1-Oxide analysis of the used materials by the XRF technique, mass %

Oxide Material	SiO_2	Al_2O_3	Fe_2O_3	CaO	MgO	MnO	SO_3	Na_2O	P_2O_5	K_2O	LOI
OPC	20.12	4.25	1.29	63.13	1.53	0.36	2.54	0.55	0.19	0.30	2.64
WSA	68.83	2.67	0.46	9.02	3.55	0.03	----	12.37	----	1.11	----

Table 2- Mineral composition of the used Type I-OPC cement wt. %

Phase Material	C_3S	β-C_2S	C_3A	C_4AF
OPC	43.01	30.00	5.65	9.58

Table 3- The batch composition of cement mixtures, mass %

Batch Material	W0	W1	W2	W3	W4	W5	Densit, g/cm^3	Blaine Finene, cm^2/g	Specific gravity
OPC	100	96	92	88	84	80	2.2215	3400	3.14
WSA	----	4	8	12	16	20	2.6546	6810	3.31
Fineness, cm^2/g	3400	3464	3561	3707	3873	4081			

2.2. Preparation of cement batches

Six cement batches were prepared from OPC and WSA as 100:0, 96:4, 92:8, 88:12, 84:16 and 80:20, which were given the symbols: W0, W1, W2, W3, W4 and W5, respectively. The blending process was mechanically made in a porcelain ball mill containing three balls for one hour to assure the complete homogeneity of all cement batches. Before casting of cement cubes, all moulds were oiled with a thin film of oil to easify the release of the cubes from the moulds during the de-moulding process. To improve the dispersion of the different cement batches, a certain percentage of Na-lignosulphonate admixture must be added to all cement mixtures with the mixing water during casting of cement pastes to avoid the agglomeration of the nanoparticles of cement powder and WSA [15,18,19]. Sodium lignosulfonate admixture (SLA) was applied due to its higher activity than other conventional ones (Fig. 1).

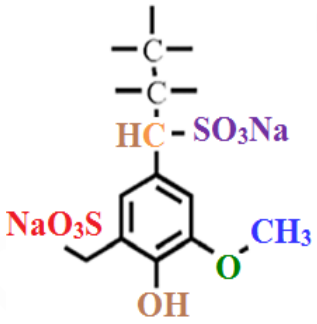

Fig. 1-The chemical formula of sodium lignosulphonate

A mechanical mixing was used for all cement mixtures using a suitable laboratory mechanical mixer in order to obtain homogenous mixtures. Firstly, the standard water of consistency [20] as well as setting time [21] of the various cement pastes were directly determined using Vicat Apparatus (Fig. 2).

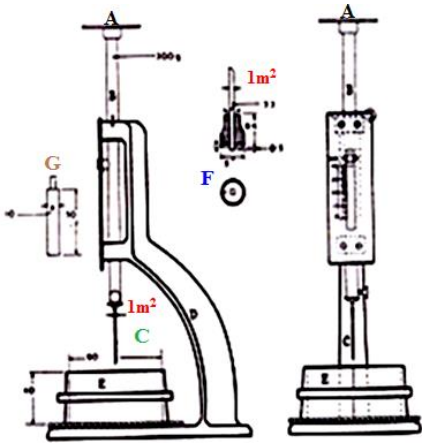

Fig. 2- Determination of water consistency and setting times by Vicat Apparatus

2.3. Methods

The water of consistency could be determined from the following relation:

$$WC, \% = A / C \times 100 \quad \text{-----} \quad (1)$$

Where, A is the amount of water taken to produce a suitable paste, C is the amount of cement mix (300 g). The initial setting time was measured by calculating the time taken from the moment at which the needle could penetrate to the paste up to 5 ml from the bottom, while the final setting time was calculated by measuring the time taken from the moment at which the water added to the cement till the final set when the impression of the needle disappeared on the surface of the pastes. During the dry mixing process, the right w/c-ratio was poured into the cement portion inside the mixer and then run the mixer for about 10 minutes at an average speed of 10 rpm in order to have a perfect homogenous mixture. During casting of the cement cube moulds, each already prepared oil mould was filled with the premixed cement composite and rammed 10 minutes to eliminate all air bubbles tapped within the mixture. The moulds were filled to the top surface and smoothed with a flat stainless steel trowel or spatula to obtain a flat smooth surface. The moulds were then casted with the prepared cement pastes using the predetermined water/cement ratio into one inch cubic stainless steel moulds (2.5 x 2.5 x 2.5 cm^3) using about 500 g cement mix, vibrated manually for three minutes and then on a mechanical vibrator for another three minutes. The surface of the moulds was smoothed using a suitable trowel or spatula. After casting all cement cubes, they were covered with a black wet sheet for the first 24 hours to prevent moisture loss. Thereafter, the moulds were kept in a humidity chamber for 24 hours under 100% relative humidity and room temperature 23 ± 1 °C. In the following day, it demoulded and soon cured under water till the time of testing at 1, 3, 7, 28 and 90 days.

At each hydrating interval, the bulk density (BD) and apparent porosity (AP) of the hardened cement pastes [13,15,16,20-22] were calculated from the following equations:

$$B.\ D, (g/cm3) = W1/(W1–W2) \times 1 \quad \text{-----} \quad (2)$$

$$A.\ P, \% = (W1 – W3)/(W1–W2) \times 100 \quad \text{-----} \quad (3)$$

Where, W1, W2 and W3 are the saturated, suspended and dry weights, respectively.

Then, the compressive strength (CS) of the various hardened cement pastes [23-25] was measured using a suitable Piston as follows:

$$CS = L\ (KN)/Sa\ (cm2)\ KN/m^2 \times 102\ (Kg/cm^2)/10.2\ (MPa) \quad \text{-------} \quad (4)$$

Where L is the load taken, Sa is the surface area. Thereafter, about 10 grams of the broken specimens from the determination of compressive strength were first well ground, dried at 105 ºC for 30 min. and then were placed in a solution mixture of 1:1 methanol: acetone to stop the hydration [23-25]. The chemically combined water content was also determined at each hydration period by heating up to 1000 °C for 30 minutes soaking time. About one gram of the sample was placed inside a crucible and first dried at 105ºC for 24 hours, and then the crucibles were placed into a furnace [26-29]. The chemically-combined water content (CWn) at each hydration age was determined as follows:

$$CWn, \% = W1\text{-}W2/W2 \times 100 \quad (5)$$

Where, CWn, W1 and W2 are combined water content, weight of sample before and after ignition, respectively.

The free CaO content (FLn) of the hydrated samples pre-dried at 105 °C for 24h was also determined. About 0.5 g sample + 40 ml ethylene glycol → heating to about 20 minutes without boiling. About 1–2 drops of ph.ph indicator were added to the filtrate and then titrated against freshly prepared 0.1N HCl until the pink colour disappeared. The 0.1 N HCl was prepared using the following equation:

$$V1 = N \times V2 \times W\ (7) \times 100/D \times P \times 1000 \quad (6)$$

Where, V1 is the volume of HCl concentration, V2 is the volume required, N is the normality required, W is the equivalent weight, D is the density of HCl concentration and P is the purity (%). The heating and titration were repeated several times until the pink colour did not appear on heating. The free lime content [14,18,27,30] was calculated from the following relation:

$$FLn, \% = (V \times 0.0033/1) \times 100 \quad (7)$$

Where, FLn is the free lime content and V is the volume of 0.1 N HCl taken on titration, respectively.

The obtained results were confirmed with the deferential thermal analysis (DTA) and scanning electron microscopy (SEM) of some selected samples. The DTA thermographs were carried out using NETZSCH Geratebae GmbH Selb, Bestell No. 348472c at a heating rate 10 °C/min. up to 1000 °C. The SEM microscopy was carried out by JEOL–JXA–840 electron analyzer at accelerating voltage of 30 KV. The fractured surfaces were fixed on Cu-kα stubs by carbon paste and then coated with a thin layer of gold.

3. RESULTS AND DISCUSSION

3.1. Chemical composition of glass powder and cement

The chemical composition of WSA in comparison with some pozzolanic materials is shown in Table 4. According to ASTM C618, 2015a [31], the sum of SiO_2+Al_2O_3 + Fe_2O_3 requirement for a standard pozzolana is 70% which is more or less that of WSA sample. The standard also sets maximum limit of SO_3 and Loss on Ignition (LOI) as 4% and 10%, respectively. As shown in Table 4, the SO_3 content of WSA sample was found well below the acceptable limit, whereas LOI was negligible. Therefore, the WSA powder is expected to be as a pozzolanic material in the cementitious system.

Table 4- Chemical composition of WSA in comparison with GbfS, SF, PFa, SCBA, SDA and SFSA

Materials Oxides	GbfS	SF	PFa	SCBA	SDA	SFSA	WSA
SiO_2	36	90.9	59.2	70.83	66.17	63.83	69.36
Al_2O_3	12	1.1	25.6	9.21	4.35	6.68	5.97
Fe_2O_3	1	1.5	2.9	1.95	2.36	2.79	2.15
CaO	38	0.7	1.1	8.16	10.06	5.46	7.28
MgO	----	0.8	0.3	1.32	4.41	6.23	1.44
Na_2O	0.3	----	0.2	0.12	0.08	0.24	0.31
K_2O	-----	-----	0.9	1.65	0.12	1.17	1.11
SO_3	8.11	0.4	0.3	1.47	0.30	1.11	1.27
P_2O_5	2.16	----	0.14	----	0.46	----	----
MnO	1.31	----	1.05	----	2.19	----	----
LOI	1.0	3.0	1.4	6.91	0.84	3.35	2.37

3.2. Physical properties

The relationship between the surface area or fineness of the OPC (W0) and the various cement batches incorporated WSA (W1-W5) is represented in Figure 3. It is clear that as the WSA content increased in the cement mix, the surface area or fineness of the whole mix increased too as shown in Table 3 and Figure 3. This is mainly due to the presence of nanograin size particles of WSA [13-15, 18].

3.3. Water of consistency and setting times

The water of consistency as well as setting times (initial and final) of the OPC (W0) and the various cement pastes containing wheat straw ash (W1-W5) were presented as a function of cement mixes in Fig. 4. The water of consistency decreased with the increase of WSA content. This is mainly attributed to the continuous decrease of the main cementing material of the cement which is responsible for the hydration process in the presence of water [18, 32-34]. The same trend was displayed with setting times, i.e. the setting times decreased with WSA content. This is principally due to the same reason mentioned before [13,18]. The WSA only reacted with the evolved Ca $(OH)_2$ from the hydration of calcium silicate phases of the cement (C_3S and β–C_2S) to produce additional CSH. This will decrease the free lime content and increase the mechanical properties as we will discuss later.

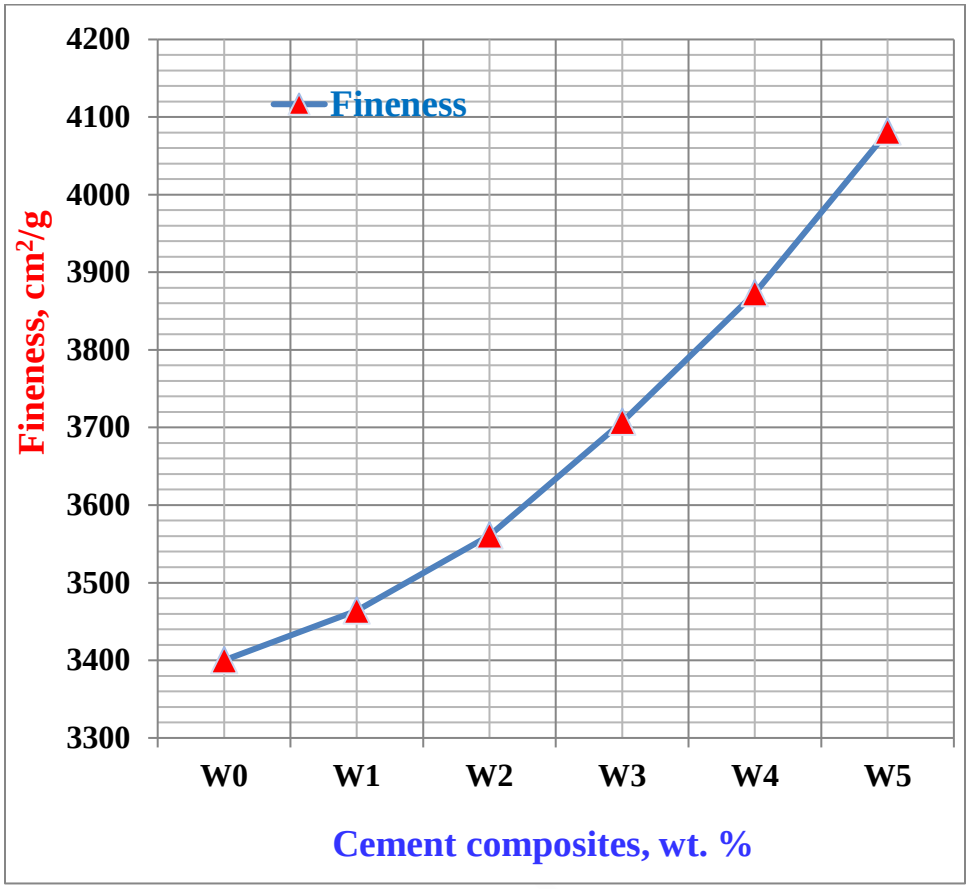

Fig. 3- Relationship between the fineness of the different cement batches containing WSA

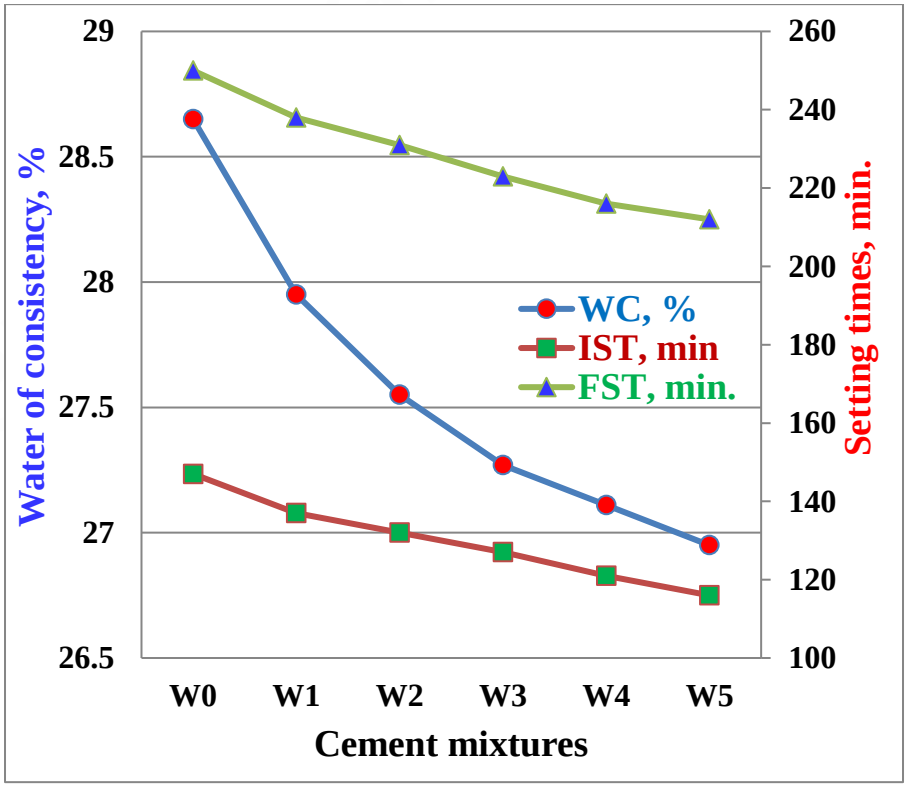

Figure 4- Water of consistency and setting times of the various cement pastes (W0-W5)

3.4. Heat of hydration

The heat of hydration of the various cement pastes containing WSA (W0-W5) is graphically plotted versus the hydration times for 1, 3, 7, 28 and 90 days in Fig. 5. Results illustrated that as soon as the various cement powder become in contact with water, the heat of hydration of the various cement pastes was started soon and then increased as the hydration time proceeded up to 90 days. This was the same trend for all cement pastes at all hydration ages. This is mainly due to the increase of the hydration rate of cement pastes. This was accompanied by the release of heat [17,22,35]. Furthermore, the rate of the resulted heat of hydration sharply enhanced at early ages up to 7 days. This is essentially attributed to the activation effect of the hydration reaction mechanism of C_3S by the very fine active nanosilica particles of WSA. At later stages (28-90 days), the rate of hydration reaction as well as the evolved heat of hydration slightly increased. This may be due to the activation action mechanism of β-C_2S by the fine WSA nanoparticles [13-15,18]. The heat of hydration enhanced as the WSA content increased only up to 16 wt % WSA (W1-W4). With any further increase of WSA (W5), lower values of heat of hydration were recorded than those of the blank (G0). This was essentially due to the dilution effect of the main binding material (OPC), and the retardation effect of the higher quantity of WSA at the expense of the OPC portion.

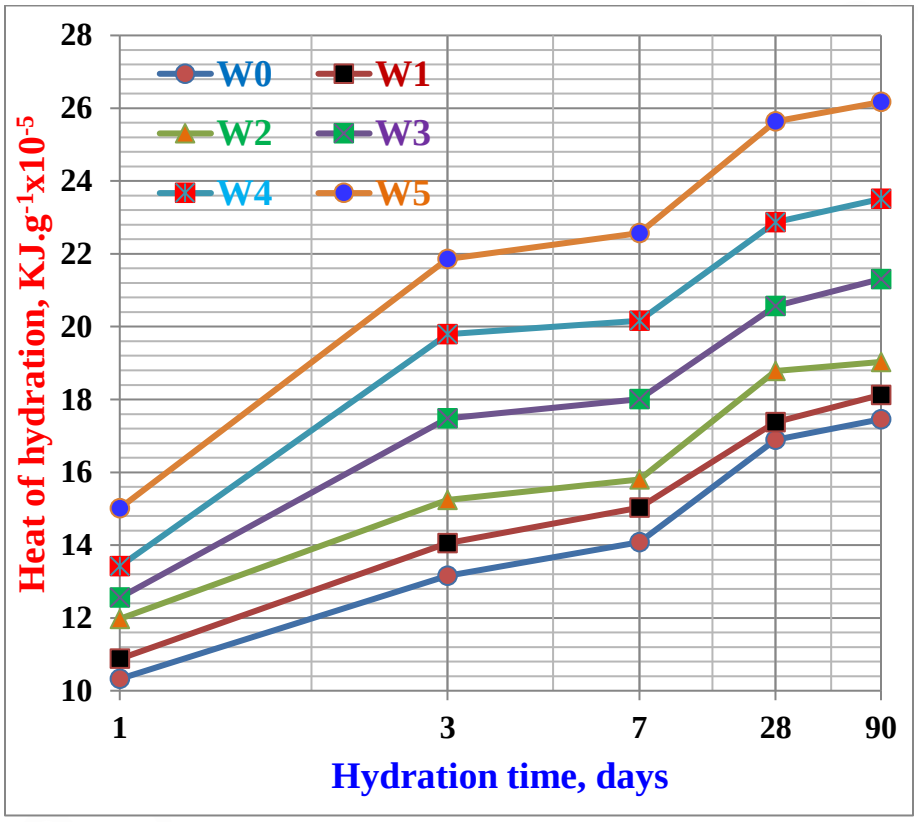

Figure 5- Heat of hydration of the various cement pastes (W0-W5) hydrated up to 90 days.

3.5. Chemically-bound water contents

The chemically-bound water contents of the various cement pastes containing WSA (W0-W5) are graphically drawn as a function of hydration times in Fig. 6. Generally, the bound water contents of all cement pastes enhanced as the hydration time progressed up to 90 days. This is mainly due to the hydration of the main cement phases, especially C_3S, C_3A and C_4AF at early ages of hydration up to 7 days, whereas β-C_2S often hydrates at later ages from 28 days onward [13,17,22]. The bound water contents slightly increased as the WSA content increased only up to 16 wt %, and then suddenly decreased sharply with further increase of WSA almost at all hydration ages, i.e. the cement blends W1, W2,W3 and W4 containing 4, 8, 12 and 16 wt % WSA, are respectively slightly higher when compared with those of the blank (W0). This is primarily due to the activation effect of the active nanosilica of the WSA [36-39]. Furthermore, the pozzolanic reactions of WSA through which the constituents of WSA could be reacted with the resulting Ca $(OH)_2$ from the hydration of C_3S at early stages of hydration and β-C_2S at later stages to produce additional CSH and/or CAH. Whereas, the bound water contents of W5 containing 20 wt. % WSA are becoming lower than those of the control mix (W0). This may be due to that the higher amounts of WSA hindered and be an obstacle for the hydration of cement phases, and the large deficiency of the main hydrating material is the main reason for the decrease of bound water contents [16,37,38,40]. Hence, it can be

concluded that the optimum WSA content could not be more than 16 wt %, i.e. the higher quantity of WSA is undesirable due to its adverse effect. Therefore, the higher amounts of WSA must be avoided because it may be hindered the hydration of cement phases.

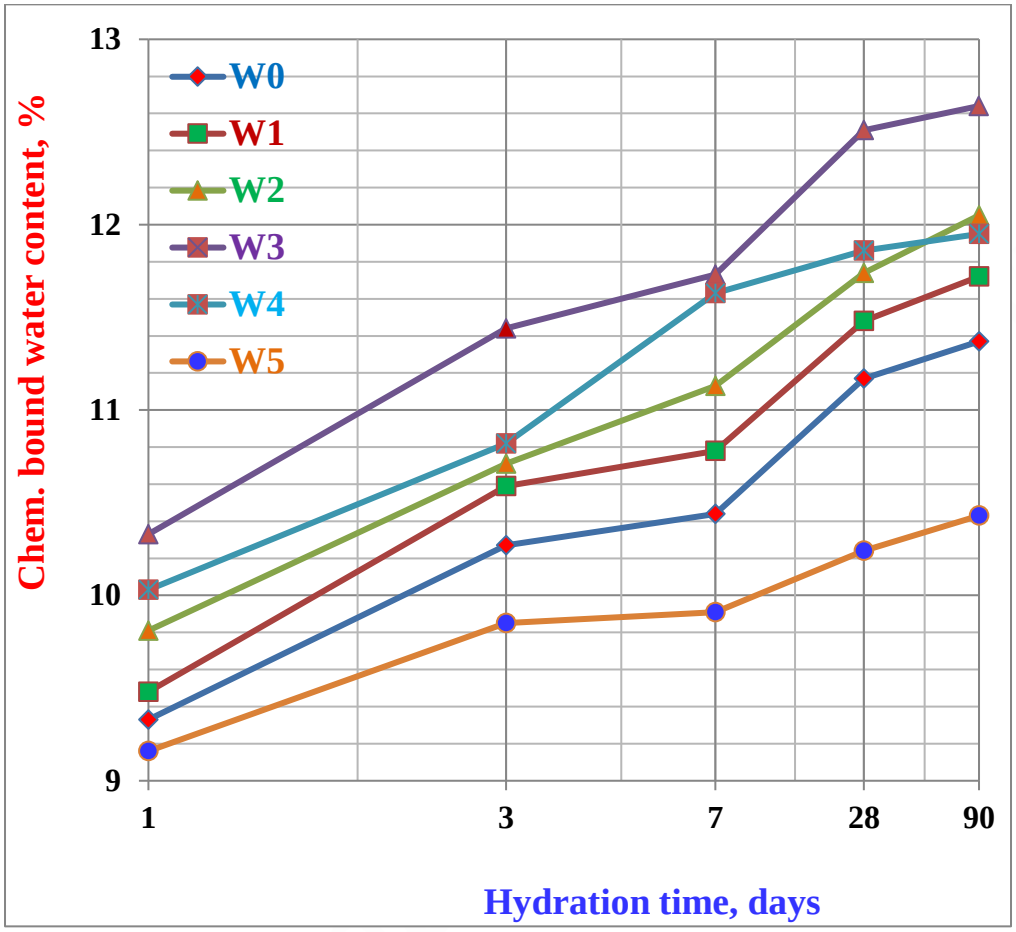

Figure 6- Chemically-bound water contents of the various cement pastes (W0-W5) hydrated up to 90 days.

3.6. Free lime content

Figure 7 indicates the free lime contents of the various cement mixes (W0-W5) hydrated up to 90 days versus hydration time. Generally, the free lime contents of the control cement pastes (W0) were gradually increased with the hydration ages up to 90 days indicating an enhancement in the rate of hydration [16,17]. This is mainly due to the hydration process of calcium silicate phases (C_3S and β-C_2S) of the cement as follows:

$$3\ C_3S + 6\ H_2O \rightarrow C_3S_2H_3 + 3\ Ca(OH)_2 \quad (8)$$

$$2\ \beta\text{-}C_2S + 4\ H_2O \rightarrow C_3S_2H_3 + Ca(OH)_2 \quad (9)$$

But, with the addition of WSA, the free lime contents of the various cement pastes (W1-W5) increased only up to 3 days, and then started to decrease. The same trend was displayed by all cement composites. The free lime contents of the various cement pastes (W1-W4) were continually decreased from 3 days up to 90 days, and therefore are being lower than those of the blank (W0) at all hydration ages [37,38]. The increase is due to the normal hydration process of the cement phases, while the decrease is due to the activation action of the active nanosilica of the WSA and its pozzolanic reactions with the resulting Ca $(OH)_2$ from the hydration of C_3S at early ages and β–C_2S at later ages of hydration in presence of water [36-39]. The cement pastes of W5 exhibited the lower values of free lime contents, while those of the blank (W0) recorded the highest.

The higher amount of WSA at the expense of the essential binding material hinders and decreases the rate of hydration of cement phases and moreover this reduces the quality of the cement. The obtained results proved that the WSA acts as a pozzolanic material, but the higher amounts of WSA must be avoided due to its adverse effect on the physical and chemical properties of the cement [35, 41-45].

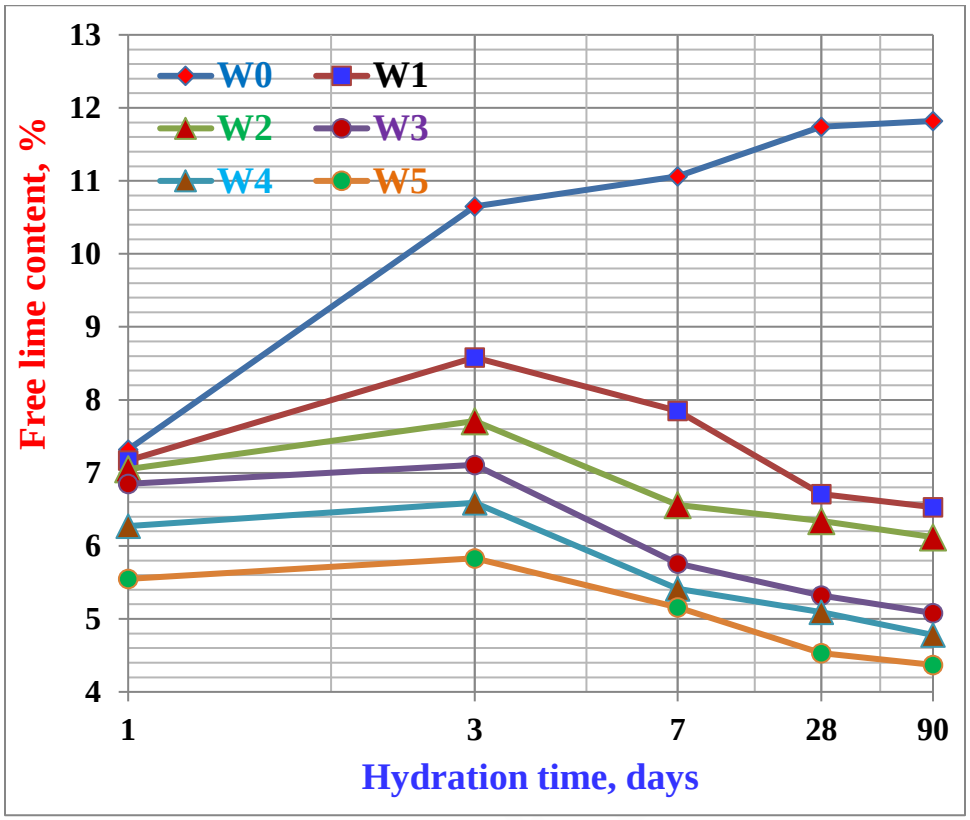

Fig. 7- Free lime contents of the various cement pastes (W0-W5) hydrated up to 90 days.

3.7. Bulk density and apparent porosity

Figures 8 and 9 demonstrate the graphs of the bulk density and apparent porosity of the various cement pastes (W0-W5) versus the hydration times. Generally, the bulk density of the various cement mixes increased as the hydration time progressed up to 90 days, while the apparent porosity decreased]16,17]. This is mainly contributed to that as the dry cement powder becomes in contact with water the hydration process started to produce CSH and/or CAH, which soon deposited in the pore structure of samples leading to a decrease in the porosity and an increase in the bulk density. As the hydration time proceeds up to 90 days, the formed hydration products increased. This in turn increased the bulk density, while the apparent porosity decreased [37]. The bulk density of the cement mixes (W1-W4) gradually increased only up to 16 wt % (W4), whereas the apparent porosity decreased, i.e. the bulk density of cement blends W1-W4 are slightly higher than those of the of the blank (W0).

This is attributed to the formation of additional calcium silicate hydrates (CSH) and/or calcium aluminate hydrates (CAH) due to the pozzolanic reactions of wheat stalk ash (WSA) with the constituents of cement through which the constituents of WSA could be reacted with the Ca $(OH)_2$ resulting from the hydration of C_3S at early stages of hydration and β-C_2S at later stages to produce additional CSH and/or CAH, and this is beside the normal hydration process of cement phases [46]. With further increase of WSA (> 16 wt %), i.e. W5, the BD started to decreased while the apparent porosity increased at all hydration times due to that the higher quantity of WSA may obstruct and hinder the hydration process, i.e. it affects negatively and decrease the rate of hydration, but it slightly benefits as a filler [28,46,47] . Hence, the incorporation of large amounts of WSA at the expense of the main binding material (W0) is undesirable due to that it was insufficient for inducing the reactions of cement with the active nanosilica of WSA. So, it could be concluded that the WSA is so beneficial to cement that it helps with the hydration process as a pozzolanic material and also as a filling material.

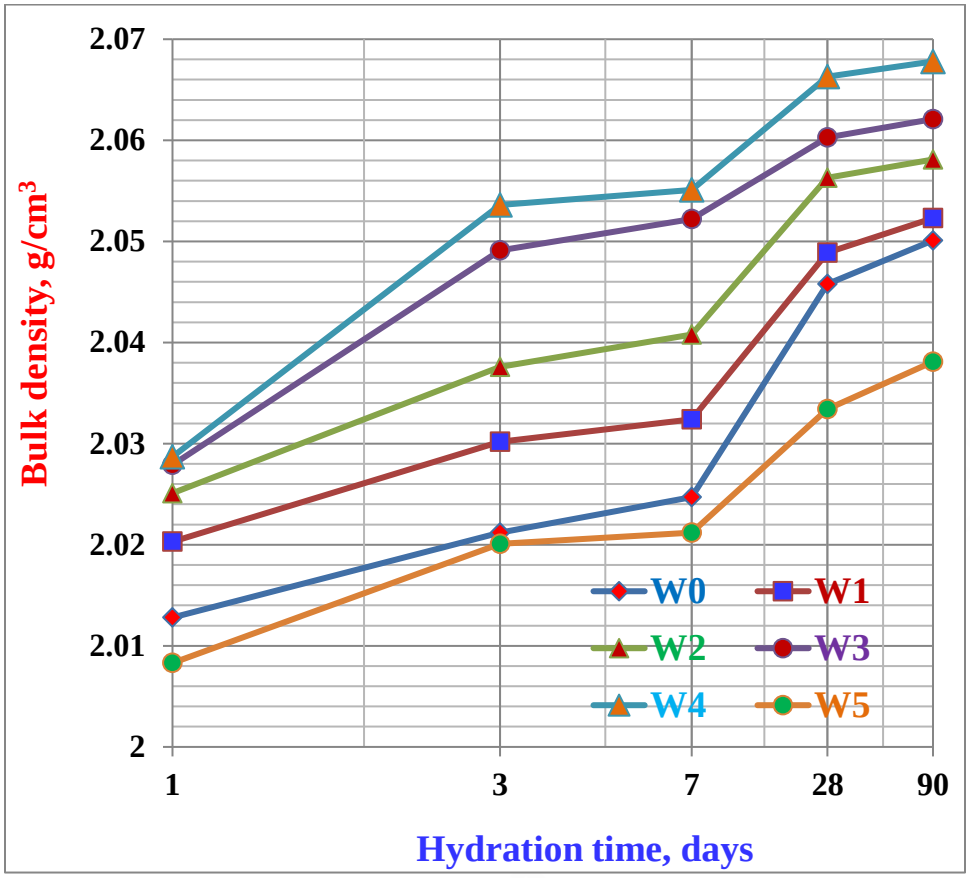

Figure 8- Bulk density of the various cement pastes (W0-W%) hydrated up to 90 days.

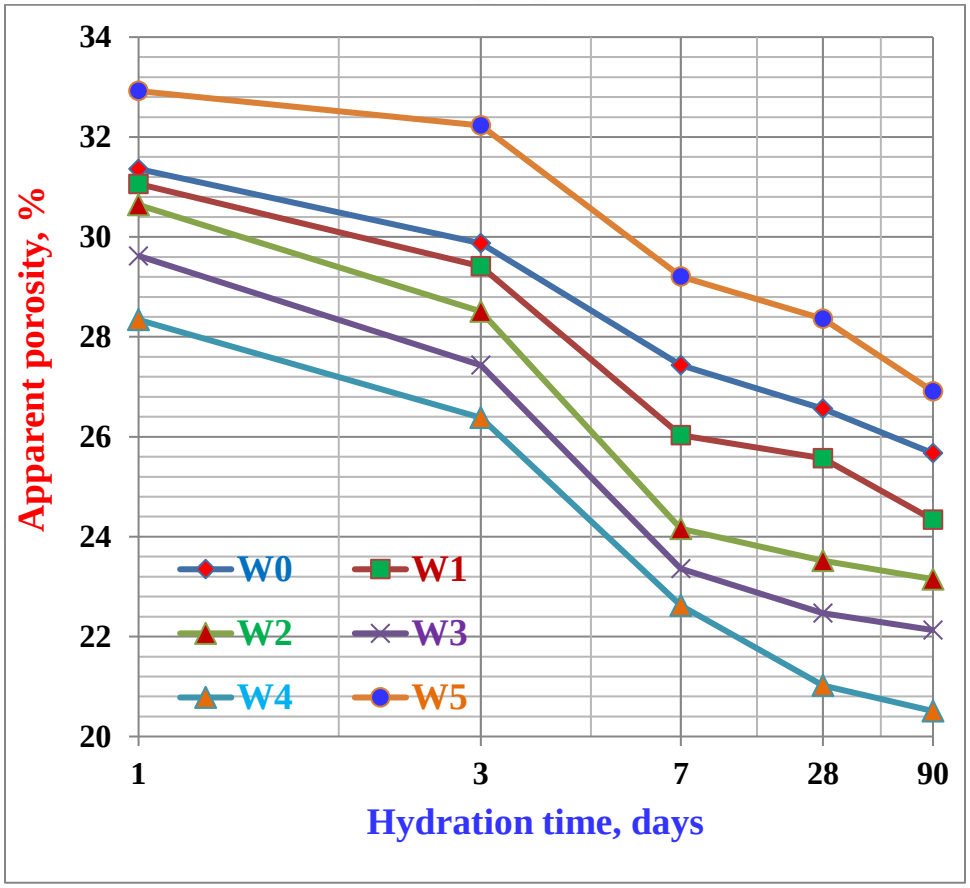

Figure 9- Apparent porosity of the various cement pastes (W0-W%) hydrated up to 90 days.

3.8. Compressive strength

It is well known that the w/c ratio of cement pastes and/or concrete affects the workability to a large extent, which in turn affects the strength of cement pastes, mortars and/or concrete [16,17,46]. Figure 10 represents the graph of the compressive strength (CS) of the various cement pastes (W0-W5) versus the hydration time up to 90 days. The compressive strength gradually improved and enhanced as the hydration period proceeded up to 90 days. This is mainly attributed to the formation of hydration products (CSH and/or CAH) that deposited into the pore structure of the hardened cement samples. This results in a decrease in the pore structure and an increase in the bulk density. This improved and enhanced the compaction of the prepared samples, besides the good dispersion by the lignosulfonate admixture and the good compaction during casting which in turn reflected positively on the compressive strength, As a result, the compressive strength increased and improved [38,40]. The CS also enhanced as the WSA content increased at all hydration times, but only up to 16 wt % WSA (W5). This is essentially due to the activation effect of the active nanosilica from WSA, and formation of more CSH that is resulting from the pozzolanic reactions of those nanosilica and nanoalumina of WSA with the free lime evolved from the hydration of C_3S and β–C_2S of cement to produce CSH and/or CAH.

On the other hand, the decrease of free lime improves the physical, chemical and mechanical properties of the hardened cement pastes and therefore the CS improved and enhanced [16,18,35,39,46]. The continuous deposition of hydration products (CSH from the normal hydration of cement phases and additional CSH from the pozzolanic reactions of WSA with the released free lime led to the segmentation of large capillary pores and nucleation sites [37-39,41,48]. By further increase of WSA > 16 wt % (W5), the CS values were suddenly decreased due to the replacing of WSA at the expense of the essential cementitious material of the cement and the higher amount of WSA stand as an obstacle against the normal hydration of cement phases. So, the rate of hydration shortened, and accordingly, this should be reflected negatively on the CS [16,17,46]. The cement mix (G) achieved the highest values of CS, whereas that of W5 exhibited the lowest. Consequently, the cement batch (W4) is the optimum cement batch. Hence, the WSA does not only improve the various characteristics of the OPC, but, it also decreases the costs of the very expensive OPC production.

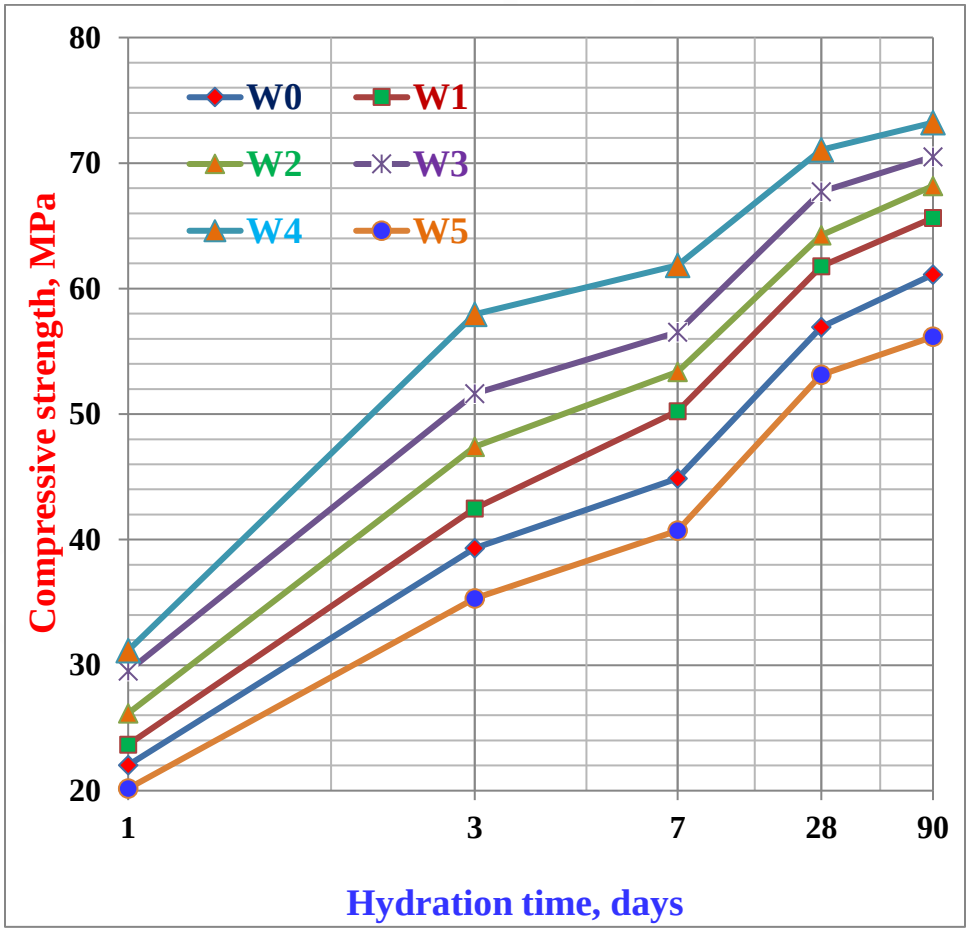

Figure 10- Compressive strength of the various cement pastes (W0-W5) hydrated up to 90 days.

3.9. DTA thermographs

Figure 11 shows the DTA thermographs of W0, W2 and W4 samples containing 0, 8 and 16 wt % WSA, respectively. The endothermic peaks at the temperature range of 94–1110 ºC and 170-181 ºC are mainly attributed to the dissociation of ettringite (C_3A. $3CaSO_4$. $32H_2O$) and C-S-H. The endothermic peak at the temperature range 486–506 ºC is essentially due to the breakdown of Ca $(OH)_2$ or free lime. The two endothermic peaks at the temperature ranges of 770–780 ºC and 785-810 ºC are certainly due to the decomposition of carbonates of various crystallinities. The endothermic peak at the temperature range of 830–915 ºC is basically due to the breakdown of sulfates. The DTA analysis proved that the presence of WSA played an vital role in the consumption of a large part from the released $Ca(OH)_2$ from the hydration process.

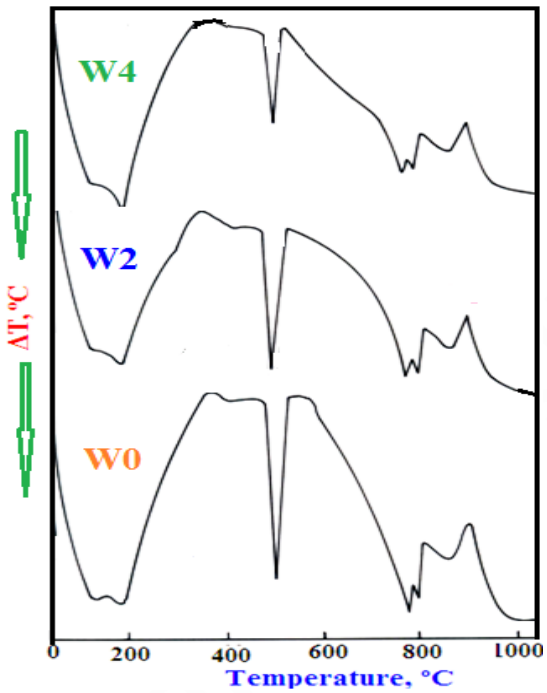

Figure 11-DTA curves of the OPC (W0), W2 and W4 cement pastes containing 0, 8 and 16 wt % WSA at 1000 °C.

3.10. Scanning electron microscopy

Figure 12 shows the scanning electron microscopy (SEM) of W0, W2 and W4 hydrated up to 28 days. The ettringite phase is obviously formed in the blank (W0) as needles-like crystals. Long and sharp crystals of CSH and/or CAH are detected with W2, while well-crystalysed big masses of CSH and/or CAH are shown with C4. Also, spots and/or pits of portlandite (free lime) are well detected in W0 and W2 samples with various levels, but they are completely disappeared in W4 sample. This proved that the addition of WSA decreased the free lime content resulting from the pozzolanic reactions of CSA with the formed Ca $(OH)_2$ due to the normal hydration of cement. Consequently, the existence of WSA in contact with the different cement phases improved and well-developed the microstructure of the cement phases.

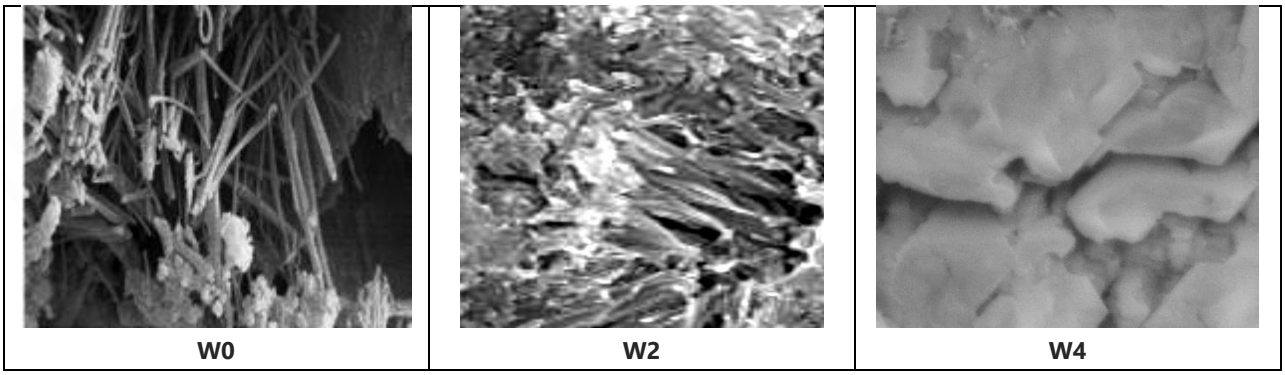

Fig. 12- SEM images of the blanck (W0) and those containing WSA (W2 and W4) hydrated up to 28 days.

4. CONCLUSIONS

Concerning the findings of the laboratory test results, the following overall conclusions could be obtained:-

1-As the active nanosilica content of WSA enhanced in the cement blends, the fineness of the whole batches increased too.

2-The water of consistency of the blank (W0) was 28.65 %, and the initial and final setting times were 147 and 250 minutes, respectively. These values tended to gradually decrease with the incorporation of WSA due to the presence of Na-lignosulphonate admixture, which it is a superplasticizer that reduces largely the mixing water.

3- The heat of hydration, chemically combined water content, bulk density and compressive strength were improved and increased gradually with the hydration ages up to 90 days. With the increase of WSA content, these properties enhanced only up to 16 wt. % (W4), and then decreased with its further increase.

4-The free lime content of the blank (W0) increased up to 90 days, while those of the various cement pastes (W1-W5) increased only up to 3 days and then decreased as the hydration time proceeded up to 90 days, i.e. the free lime contents are becoming lower than those of the blank.

5-The apparent porosity were declined and reduced with the replacing up to 16 wt. % WSA (W4), and then increased with further increase of more than 16 wt % WSA.

6-Improving and enhancing of all properties of the cement could be achieved by the pozzolanic reactions leading to the reduction of Ca $(OH)_2$ which is coming from the hydration of C_3S and β–C_2S phases of the cement, and by increasing the deposition sites of the hydration products. Moreover, the activating and filling effects of the active nanosilica of the WSA initiated and promoted these properties.

7-The addition of 12 % GW (G4) to Portland cement could be applied without any adverse effects on the physical, chemical and mechanical properties of Portland cement. Therefore, it was selected to be the optimum batch.

8-The incorporation of the Na-lignosulphonate admixture is the mean cause responsible for the modification of the hardened cement pastes.

9-The DTA analysis proved that the free lime content was consumed by WSA, i.e. it acts as a pozzolanic and/or filler material.

10-The SEM images showed that the presence of WSA with the cement phases reflected positively on the microstructure of the cement phases.

Acknowledgement

Author wish to express their deep thanks for National Research Centre for helping to obtain materials, processing, preparing, molding and measuring all of the obtained data of the study, and moreover for financial assistance.

Conflict of interests

There is no conflict of interest among the authors.

Funding

There is no direct funding for this project.

Peer-review

External peer-review was done through double-blind method.

Data and materials availability

All data associated with this study are present in the paper.

REFERENCE

1. Darweesh HHM; Kenawy SH (2020), Light-weight highly porous building bricks from Sawdust, Indian Journal of Engineering, 17, 37,193-2030.
2. Heniegala, AM; Ramadanb,MA; Naguibc, A; Agwad, IS (2020), Study on properties of clay brick incorporating sludge of water treatment plant and agriculture waste, Case Studies in Construction Materials 13.
3. Darweesh HHM (2018), Nanomaterials: classification and properties—Part I. J Nanosci 1(1):1–11.
4. Darweesh HHM (2018), Nanoceramics: materials, properties, methods and applications—Part II. J Nanosci 1(1):40–66.
5. Eisentraut, ABA (2012), Technology Roadmap Bioenergy for Heat and Power. International Energy Agency.
6. Rukzon S; Chindaprasirt P (2012), Utilization of bagasse ash in high-strength concrete, Materials & Design, 34, 45–50.

7. Aksogan, O; Binici, H; Ortlek, E (2016), Durability of concrete made by partial replacement of fine aggregate by colemanite and barite and cement by ashes of corn stalk, wheat straw and sunflower stalk ashes. Construction and Building Materials, 106: 253-263.
8. Zhang, H; Hu, J; Qi, Y; Li, C; Chen, J; Wang, X; He, J; Wang, S; Hao, J; Zhang, L, Zhang,Y, Li, R; Wang, S; Chai, F (2017), Emission characterization, environmental impact, and control measure of PM2.5 emitted from agricultural crop residue burning in China. Journal of Cleaner Production, 149: 629-635.
9. Abdulkadir, T.S.; Oyejobi, D.O.; Lawal, A.A. (2014), *Evaluation of Sugarcane Bagasse Ash as a Replacement for Cement in Concrete, Works* Acta Tehnica Corviniensis – Bulletin of Engineering (Ilorin: University of Ilorin), 71–76.
10. Raheem, AA; Aedokun; SI; Adeyinka, EA; Adewole, BV (2017), Application of cornstalk ash as partial replacement for cement in the production of interlocking paving stones,International Journal of Engineering Research in Africa, 30: 85-93.
11. Binici, H; Ortlek E (2015), Engineering properties of concrete made with cholemanite, barite, corn stalk, wheat straw and sunflower stalk ash. European Journal of Engineering and Technology, 3.
12. Fan WJ; Wang XY; Park KP (2015), Evaluation of the Chemical and Mechanical Properties of Hardening High Calcium Fly Ash Blended Concrete, Materials, 8, 5933-5952.
13. Darweesh HHM; Abo El-Suoud MR (2018), Saw dust ash substitution for cement pastes-Part I", American j. of Construction and Building Materials, 2, 1, 1-9.
14. Darweesh HHM; Abo El-Suoud MR (2019), Influence of sugarcane bagasse ash substitution on Portland cement characteristics, Indian Journal of Engineering, 16, 252-266.
15. Darweesh HHM; Abo El-Suoud MR (2020), Palm Ash as a Pozzolanic Material for Portland Cement Pastes, To Chemistry Journal, 4, 72-85.
16. Neville, AM (2011), Properties of Concrete, 5th Edn, Longman Essex (UK), ISBN: 978-0-273-75580-7 (pbk.).
17. Hewlett PC; Liska M (2017), Lea's Chemistry of Cement and Concrete, 5th ed., Edward Arnold Ltd., London, England Google Scholar
18. Darweesh, HHM (2020), Characteristics of Portland Cement Pastes Blended with Silica Nanoparticles, To Chemistry, 5, 1-14.
19. Topçu, I B; Ateşin, Ö. (2016), Effect of high dosage lignosulphonate and naphthalene sulphonate based plasticizer usage on micro concrete properties. *Construction and Building Materials*, 120:189–197.
20. ASTM-C187-86 (1993), Standard Test Method for Normal Consistency of hydraulic Cement, 148-150.
21. ASTM-C191-92 (1993), Standard Test Method for Setting Time of Hydraulic Cement, 866-868.
22. Darweesh, HHM and Nagieb, A (2007), Hydration and micro-structure of Portland/Calcined Bentonite Blended Cement Pastes, *Indian Journal of Chemical Technology,* 14 301-307.
23. ASTM- C170-90 (1993), Standard Test Method for Compressive Strength of Dimension Stone", 828-830.
24. ASTM-C109M (2013), Standard Test Method for Compressive Strength of Hydraulic Cement Mortars (Using 2-in. Or [50-mm] Cube Specimens), Annual Book of ASTM Standards. ASTM International, West Conshohocken, PA.
25. ASTM C39 (2016) Standard Test Method for Compressive Strength of Cylindrical Concrete Specimens. ASTM International, West Conshohocken, USA.
26. Mohammed T U, Ahmed T, Apurbo S M, Mallick TA, Shahriar F, Munim A, Awal AA (2017). Influence of chemical admixtures on fresh and hardened properties of prolonged mixed concrete. *Advances in Materials Science and Engineering*. 1-11.
27. Karim MR, Zain MFM, Jamil M (2012), Strength of Mortar and Concrete as Influenced by Rice Husk Ash: A Review, *World Applied Sciences Journal,* 19.10, 1501-1513.
28. Siddique R (2011), Properties of self-compacting concrete containing class F fly ash. Mater Des, 32:1501–7.
29. Darweesh HHM (2014) Utilization of Perlite Rock in Blended Cement-Part I: Physicomechanical properties, Direct Research Journal of Chemistry and Material Sciences 2354-4163.
30. Darweesh, HHM (2012), Setting, hardening and strength properties of cement pastes with zeolite alone or in combination with slag, Interceram Intern. (Intern Cer Review), Germany, Vol. 1, 52-57.
31. ASTM C618a (2015) Specification for Coal Fly Ash and Raw or Calcined Natural Pozzolan for Use in Concrete. ASTM International, West Conshohocken, USA.
32. Imbabi MS, Carrigan C, McKenna S (2012) Trends and developments in green cement and concrete technology. Int. J. Sustain. Built Environ. 1, 194–216.
33. Darweesh HHM (2017), Geopolymer cements from slag, fly ash and silica fume activated with sodium hydroxide and water glass, Interceram International", 6, 1, 226-231.
34. Rashed AM (2014) Recycled waste glass as fine aggregate replacement in cementitious materials based on Portland cement. Constr. Build. Mater. 72, 340–357.
35. Heikal M, Ali Al, Ismail MN, Awad S, Ibrahim NS (2014) Behavior of composite cement pastes containing silica nano-particles at elevated temperature, Const. Build. Mater., 70. 339-350.
36. Aleem SAE, Heikal M, Morsi WM (2015) Hydration characteristic, thermal expansion and microstructure of

cement containing nano-silica, Const. Buil. Mater, 59. 151-160.

37. Darweesh HHM, Abo-El-Suoud MR (2015), Quaternary Cement Composites Containing Some Industrial By-products to Avoid the Environmental Pollution, EC Chemistry, 2, 1, 78-91.
38. Darweesh HHM (2017) Mortar Composites Based on Industrial Wastes, International Journal of Materials Lifetime, 3, 1, 1-8.
39. Sadiqul Islam GM, Rahman MH, Kazi N (2017) Waste glass powder as partial replacement of cement for sustainable concrete practice, International Journal of Sustainable Built Environment, 6, 37–44
40. Topçu, I B; Ateşin, Ö. (2016), Effect of high dosage lignosulphonate and naphthalene sulphonate based plasticizer usage on micro concrete properties. *Construction and Building Materials*, 120:189–197.
41. Amin M, Abu El-Hassan K (2015), Effect of using different types of nano materials on mechanical properties of high strength concrete, Constr. Build. Mater., 80, 116–124.
42. Stefanidou M, Papayianni I (2012), Influence of nano-SiO_2 on the Portland cement pastes, Compos. Part B-Eng. 43, 2706–2710.
43. Nazari A, Riahi S, Riahi S, Shamekhi SF, Khademno A (2010), Influence of Al_2O_3 nanoparticles on the compressive strength and workability of blended concrete, Journal of American Science, 6, 6-9.
44. Givi AN, Rashid SA, Aziz FNA, Salleh MAM (2010), Experimental investigation of the size effects of SiO_2 nano-particles on the mechanical properties of binary blended concrete, Composites Part B: Engineering, 41, 673-677.
45. Ibrahim NS, Heikal M, Ismail MN (2015), Physico-mechanical, microstructure characteristics and fire resistance of cement pastes containing Al_2O_3 nano-particles, Const. Build. Mater., 91, 232-242.
46. Rashad MA (2015) A brief on high-volume Class F fly ash as cement replacement – a guide for civil engineer. Int. J. Sustain. Built Environ. 4, 278–306.
47. Garrett TD, Cardenas HE, Lynam JG (2020) Sugarcane bagasse and rice husk ash pozzolans: Cement strength and corrosion effects when using saltwater. Current Research in Green and Sustainable Chemistry 1-2:7-13.
48. Darweesh HHM (2014) Utilization of Perlite Rock in Blended Cement-Part I: Physicomechanical properties, Direct Research Journal of Chemistry and Material Sciences 2354-4163.